Gravitational and magnetic field effects on the dynamical diffraction of neutrons

S. A. Werner
Physics Department and Research Reactor Facility, University of Missouri, Columbia, Missouri 65211
(Received 10 August 1979)

This paper examines in detail the effect of an external force field on the diffraction of neutrons by a perfect crystal. The theoretical connection of this problem with the propagation of x rays in a strained crystal, and with the motion of band electrons in a crystal under the influence of an applied electric field is described. Two methods of solution are utilized: (a) an eikonal (WKB) approach which is analogous to the method used by Kato in discussing the x-ray strain problem, and (b) a coupled-partial-differential-equation approach, which is analogous to the Takagi-Taupin method of solving the x-ray strain problem. Extensive numerical examples are given.

I. INTRODUCTION

Since the first observation of the Pendellösung fringe structure in neutron diffraction about 10 years ago by Shull,[1] interest in the application of the dynamical theory of diffraction to the neutron-scattering case has continuously increased.[2] In recent years this interest has been considerably enhanced as a result of the successful application of the Bonse-Hart x-ray interferometer[3] to neutron interferometry.[4] This device has been used to carry out precision measurements of neutron-scattering lengths,[5] to observe gravitationally induced quantum interference,[6] to observe the change of sign of the neutron wave function in a 2π precession,[7] and to detect the effect of Earth's rotation on the quantum-mechanical phase of the neutron.[8] No attention has yet been directed to the effect of gravity (or of a magnetic field) on the propagation of neutrons within the perfect, single-crystal silicon slabs from which the interferometer is constructed. It is the purpose of this paper to examine this problem in detail.

In order to focus on a specific problem, we consider the symmetric transmission-Laue geometry shown in Fig. 1. Generalizing to asymmetric geometries is straightforward. A nominally monoenergetic beam of neutrons of wave vector $\vec{k}_0$ is incident on the crystal oriented at the Bragg-reflection condition for a given reciprocal-lattice vector $\vec{G}$. The incident beam is defined in space by a slit which is small in comparison to the crystal thickness T, but large in comparison to the neutron wavelength. In addition to the periodic potential $V(\vec{r})$ of the crystal lattice which gives rise to the Bragg-scattered beam, the neutron is acted upon by the gravitational potential $m\vec{g}\cdot\vec{r}$ (where m is the neutron mass, and $\vec{g}$ is the acceleration due to gravity). From the standard results of the dynamical theory of diffraction, we know that under conditions of Bragg reflection the incident neutron wave splits up into two new coherent wave fields ψ_α and ψ_β inside the crystal. At the exact Bragg condition the neutron density corresponding to ψ_α has nodes at the atomic planes, while the neutron density corresponding to ψ_β has nodes between the atomic planes, as shown in Fig. 1. This perfect registry of these wave fields with respect to the atomic planes leads to the anomalous-transmission effect[9] (Borrmann effect) familiar in x-ray diffraction. However, with the addition of the gravitational potential $m\vec{g}\cdot\vec{r}$ to the Hamiltonian, we know that the phase (wave vector) of the neutron wave must be continuously shifted as the neutron moves through a macroscopic crystal, thus spoiling the perfect registry of the neutron wave function with the crystal lattice.

Qualitatively, one can understand that there are some important effects. For example, in an absorbing crystal the shift of phase of the standing-wave pattern corresponding to ψ_α in Fig. 1 resulting from

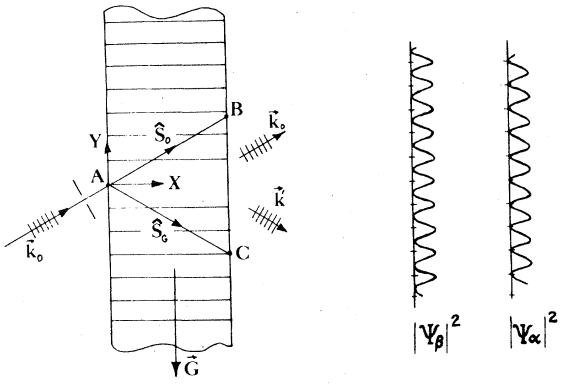

FIG. 1. Symmetric Laue-transmission geometry. The incident plane wave, of wave vector $\vec{k}_0$, is restricted laterally by a narrow slit. The triangle ABC is the Borrmann triangle. Diffracted intensity originates from only this region of the crystal. This figure also shows the neutron density corresponding to the α and β branches of the dispersion surface at the exact Bragg condition.

the gravitational field will lead to increased absorption of this wave field. That is, one expects that "turning on" the gravitational field will induce *enhanced neutron-nuclear absorption* of Bragg-reflecting neutrons. In addition, incident neutrons having wave vectors $\vec{k}_0$ oriented slightly off the exact Bragg condition at the entrant surface of the crystal will be shifted either closer to, or farther away from, the Bragg condition as they propagate deeper into the crystal under the influence of gravity. This effect will tend to increase the diffracted beam intensity, while the dephasing of the perfect registry of the wave field with the lattice will tend to decrease the diffracted beam intensity due to absorption. From these qualitative remarks it is clear that a quantitative calculation is necessary to even predict the sign of the effect of gravity on the diffracted intensity.

We remark at the outset that the problem we are considering here is directly analogous to two other fundamental problems in solid-state physics:

(i) The motion of band electrons under the influence of an external electric field $\vec{E}$: In addition to the periodic potential of the crystal lattice, the term

$$V_{\text{elect}} = e\vec{E}\cdot\vec{r} \tag{1}$$

must be added to the Hamiltonian. Thus, there is a close connection of the gravitational problem under consideration here and the Stark-Wannier ladder effect, considered first by Wannier.[10]

(ii) The effect of strain on the propagation of x rays in perfect crystals: This problem has been considered in considerable detail by Kato.[11] In a uniformly strained crystal the phasing of the x-ray (neutron) wave fields relative to the lattice is progressively changed by moving the lattice plane (due to strain) relative to the x-ray wave field. For neutrons propagating through a thick crystal under the influence of gravity, the relative phasing is shifted by a gradual change of the period of the neutron wave itself. On the basis of these considerations one might expect that the mathematical problem for these two, physically quite different situations, is similar. We find that this is, in fact, the case.

If a neutron propagates in a perfect crystal lattice under the influence of an external magnetic field having a constant gradient, the neutron will feel a uniform force given by

$$\vec{F}_{\text{mag}} = \vec{\nabla}(\vec{\mu}_n\cdot\vec{B}) \ , \tag{2}$$

where $\vec{\mu}_n$ is the neutron magnetic moment and $\vec{B}(\vec{r})$ is the magnetic induction field. It is clear that the effect of a gravitational field on the dynamical diffraction of neutrons must be similar to the effect of a gradient magnetic field if we replace $\vec{g}$ by $\vec{F}_{\text{mag}}/m$. A magnetic-field gradient of 170 G/cm produces an acceleration equivalent to $g = 980$ cm/s^2. Of course, care must be exercised in keeping track of the two spin states of the neutron.

II. NEUTRON SCHRÖDINGER EQUATION

The Schrödinger equation for the neutron inside a crystal, acted upon by the gravitational field of the Earth, is

$$[(-\hbar^2/2m)\nabla^2 + V(\vec{r}) + m\vec{g}\cdot\vec{r}]\psi = E_0\psi \ , \tag{3}$$

where E_0 is the incident kinetic energy of the neutron at point A in Fig. 1, and $V(\vec{r})$ is the periodic interaction potential energy of the neutron with the lattice. We have set the gravitational potential energy equal to zero at point A. Defining

$$k_0^2 = \frac{2m}{\hbar^2}E_0 \tag{4}$$

and

$$v(\vec{r}) = \frac{2m}{\hbar^2}V(\vec{r}) \ , \tag{5}$$

we can write Eq. (3) as

$$\nabla^2\psi - v\psi - \frac{2m^2\vec{g}\cdot\vec{r}}{\hbar^2}\psi + k_0^2\psi = 0 \ . \tag{6}$$

In the absence of the gravitational potential, the standard method of solution of Eq. (6) involves expanding the periodic potential in a Fourier series

$$v(\vec{r}) = \sum_{\vec{G}} v_{\vec{G}} e^{i\vec{G}\cdot\vec{r}} \tag{7}$$

and the neutron wave function in Bloch functions

$$\psi(\vec{r}) = \sum_{(\vec{G})} \psi_{\vec{G}} \exp(i\vec{K}_0\cdot\vec{r} + i\vec{G}\cdot\vec{r}) \ . \tag{8}$$

The vectors $\vec{G}$ are the reciprocal lattice vectors. Physically, it is clear that the main effect of adding the gravitational potential to the Hamiltonian will be to cause a gradual change of the internal wave vector $\vec{K}_0$ as a function of position within the crystal. It is reasonable to assume that Eq. (8) will be a solution of Eq. (6) locally.

Under conditions in which only one reciprocal-lattice vector $\vec{G}$ is on, or near, the Ewald sphere of reflection, only two wave amplitudes, namely ψ_0 and ψ_G, will be large. Thus, we expect that the solution of Eq. (6) must be of the form

$$\psi = \psi_0 e^{i\vec{K}_0\cdot\vec{r}} + \psi_G e^{i\vec{K}_G\cdot\vec{r}} \ , \tag{9}$$

where

$$\vec{K}_G = \vec{K}_0 + \vec{G} \ . \tag{10}$$

In the absence of the gravitational field, the wave amplitude ψ_0 and ψ_G, and the wave vectors $\vec{K}_0$ and $\vec{K}_G$ are constant, independent of position. With the addition of the gravitational potential to the Hamiltonian, it is apparent that this can no longer be the case. There are two approaches which can be followed:

a. Eikonal method. This is the method followed by Kato[11] in treating the x-ray strain problem. The basic ideas of the technique were first developed by Penning and Polder.[12] The gradual shift of phase of the wave function ψ is obtained by allowing the wave vector $\vec{K}_0$ to be weakly spatially dependent, and ignoring the gradients of ψ_0 and ψ_G locally.

b. Coupled-partial-differential-equation method. This method was developed by Takagi[13] and Taupin[14] to analyze the effects of strain in the dynamical diffraction of x rays. In this approach, the wave vector $\vec{K}_0$ is set equal to the index-of-refraction-modified value of the incident wave vector $\vec{k}_0$, and the wave amplitudes ψ_0 and ψ_G are allowed to be locally position dependent.

In the next section we will pursue the eikonal approach to understand the basic features of the effect of gravity on the dynamical diffraction of neutrons. Then in Sec. IV we will derive and solve a pair of coupled differential equations analogous to the Takagi-Taupin equations.

III. EIKONAL METHOD

In a local region of the crystal (large in comparison to the unit cell dimensions) we assume that the gradients of the wave vectors and wave amplitudes are small. Under this assumption, we find that substitution of Eqs. (7) and (8) into the wave equation (6) requires

$$\psi_{\vec{G}'}\left[k_0^2-(\vec{K}_0+\vec{G}')^2-\frac{m^2\vec{g}\cdot\vec{r}}{\hbar^2}\right]=\sum_{\vec{G}''}v_{\vec{G}'-\vec{G}''}\psi_{\vec{G}''}\ . \tag{11}$$

If we further assume that the external incident wave vector $\vec{k}_0$ is oriented very close to the Bragg condition for only one particular reciprocal lattice vector (call it $\vec{G}$), only two wave amplitudes ψ_0 and ψ_G will be large. Thus, the above infinite set of equations reduces to a pair of linear algebraic equations:

$$(Q^2-K_0^2)\psi_0-v_{-G}\psi_G=0 \tag{12a}$$

and

$$-v_G\psi_0+(Q^2-K_G^2)\psi_G=0\ , \tag{12b}$$

where for simplicity in notation we have dropped the vector sign over $\vec{G}$ in the subscripts. The internal diffracted wave vector $\vec{K}_G$ is given by Eq. (10), and

$$Q^2=k_0^2-v_0-\frac{2m^2\vec{g}\cdot\vec{r}}{\hbar^2}\ . \tag{13}$$

These equations appear to be the standard two-beam dynamical-diffraction equations, except that here the wave vectors $\vec{K}_0$ and $\vec{K}_G$ depend upon position $\vec{r}$. The wave amplitudes ψ_0 and ψ_G will also depend upon position. At first sight, this would appear to contradict our original assumption. However, the approximation involved here requires only that $\vec{\nabla}\psi_G \ll \vec{K}_G\psi_G$. We will see that this condition is generally easily satisfied.

A. Dispersion surfaces

For a nontrivial solution of Eqs. (12) to exist, the determinant of the coefficients of ψ_0 and ψ_G must be equal to zero, namely,

$$(Q-K_0)(Q-K_G)=v_Gv_{-G}\ , \tag{14}$$

where

$$v_G=v_G/2k_0\ . \tag{15}$$

In writing Eq. (14) we have made the approximations

$$Q+K_0\approx 2k_0 \text{ and } Q+K_G\approx 2k_0\ , \tag{16}$$

which we can easily justify numerically. Equation (14) gives the locus of the allowed values of the internal wave vector $\vec{K}_0$. In the absence of absorption, $\vec{K}_0$ will be real, and the solutions of Eq. (14) can be constructed geometrically in $\vec{k}$ space, as is well known. This procedure gives rise to two hyperbolic dispersion surfaces as shown in Fig. 2. The diameter D of these hyperbolas (distance between them) is very small compared to the incident wave vector $\vec{k}_0$. Although, strictly speaking, the asymptotes of these surfaces are spheres of radius Q about the origin O of reciprocal space and the reciprocal-lattice point G,

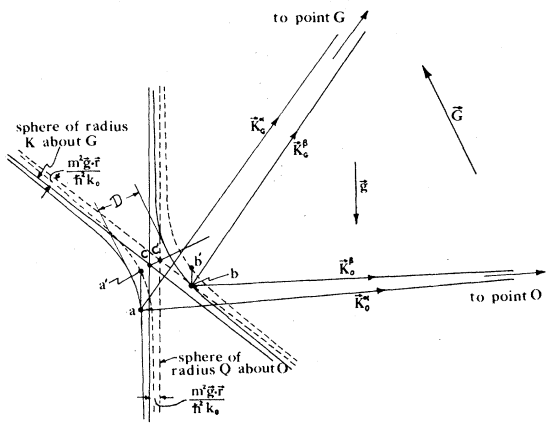

FIG. 2. The diagram shows the dispersion surfaces at the entrant point A (solid hyperbolas) and the shifted dispersion surfaces at a point r (dashed hyperbolas). At $\vec{r}=0$ (point A in Fig. 1), the dispersion surfaces are asymptotic to spheres of radius $K=k_0-\frac{1}{2}(v_0/k_0)$ drawn with centers at O and G. At a point $\vec{r}\neq 0$, these surfaces are asymptotic to spheres of radius $Q=K-m^2\vec{g}\cdot\vec{r}/\hbar^2k_0$ drawn with centers at O and G.

strongly diffracted waves will only occur for wave vectors $\vec{K}_0$ near the center C of these dispersion surfaces, and the asymptotes can be represented by planar surfaces in this region. Because the radius Q of the asymptotic surfaces depends upon position within the crystal, as given by Eq. (13), the center of the dispersion surfaces will move as a function of position $\vec{r}$. However, the diameter D and the shape of the disperison surfaces will remain constant to very high order of approximation. The net effect of gravity on the dispersion surfaces is to shift them "rigidly" in the direction CC' toward the reciprocal-lattice vector $\vec{G}$. This shift is given by $-m^2\vec{g}\cdot\vec{r}/k_0\hbar^2$, as shown in Fig. 2, since

$$Q \approx k_0 - \frac{v_0}{2k_0} - m^2\vec{g}\cdot\vec{r}/\hbar^2 k_0 \ . \tag{17}$$

B. Tie points and tie-point migration

When a neutron of incident wave vector $\vec{k}_0$ first enters the crystal at point A, the incident plane wave given by

$$\psi_{\rm inc} = \Phi \exp(i\vec{k}_0\cdot\vec{r}) \tag{18}$$

splits up into two new wave fields ψ_α and ψ_β corresponding to the α and β branches of the dispersion surfaces. The excited internal waves will have wave vectors $\vec{K}_0^\alpha$ and $\vec{K}_0^\beta$, which differ from $\vec{k}_0$ by a wave vector directed along the normal $\vec{N}$ to the entrance surface, namely,

$$\vec{K}_0^\gamma = \vec{k}_0 + \vec{N}_0^\gamma \ . \tag{19}$$

(Here γ means either α or β.) This condition must be met in order to achieve phase matching of the neutron wave function across the entrance surface. Two tie points (shown as points a and b in Fig. 2) are selected for each incident wave vector $\vec{k}_0$, one on the α branch and one on the β branch. As the neutron propagates into the crystal to a position given by the vector $\vec{r}$, the dispersion surfaces shift due to the influence of gravity, and the tie points must also shift. The question then is: How do the tie points migrate? It is clear that the change in the internal wave vectors can only occur in a direction normal to the planes of constant gravitational potential, that is along $\vec{g}$. Thus, the tie point a moves to a', and the tie point b moves to b'. However, how do we know the position $\vec{r}$ of the neutron which entered the crystal at point A as a plane wave of wave vector $\vec{k}_0$? We can answer this question using differential geometry.

C. Neutron trajectories

We will now derive the differential equation describing the neutron trajectory corresponding to a given incident wave vector $\vec{k}_0$, or equivalently, corresponding to a given initial tie point. Consider first an initial tie point b at $\vec{r}=0$ on the β branch of the dispersion surface as shown in Fig. 3. The neutron follows some trajectory given by the local direction of the current density $\vec{j}$, which is normal to the β branch of the dispersion surface at point b.[9] At some point $\vec{r}$, the dispersion surface has shifted to the right (in Fig. 3) by an amount

$$\Gamma = \frac{m^2\vec{g}\cdot\vec{r}}{\hbar^2 k_0 \cos\theta_B} \ , \tag{20}$$

where θ_B is the nominal Bragg angle. The tie point is now b', and the local direction of propagation is normal to the dispersion surface at this point. As the neutron propagates a differential distance $d\vec{r}$ further into the crystal, the dispersion surface moves a differential distance $d\Gamma$ to the right (in Fig. 3), so that the new tie point is b''. It is clear from this diagram that the neutron trajectory is curved. The differential equation describing the trajectory will be (at least) of second order. We need first to write an expression for the local normal to the dispersion surface at each tie point b as it migrates. This is most easily done by first writing the equation for the dispersion surface [Eq. (14)] in the orthogonal coordinates x_k, y_k shown in Fig. 3. The coordinates of a given tie point are specified by the scalar wave-vector differences $Q-K_0$ and $Q-K_G$. By geometry we can derive the transformation equations between these variables. The results are

$$Q - K_G = (x_k - \Gamma)\cos\theta_B + y_k \sin\theta_B \tag{21a}$$

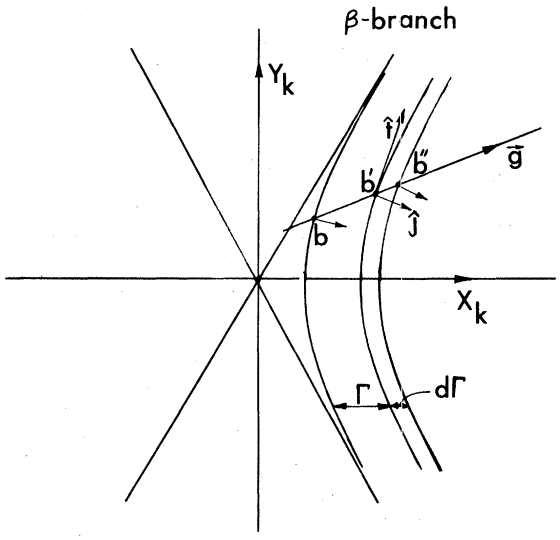

FIG. 3. β branch of the dispersion surface showing the orthogonal $\vec{k}$-space coordiantes x_k, y_k. This diagram shows how a given tie point b migrates due to gravity as the neutron moves from the entrant point A ($\vec{r}=0$) to a new point $\vec{r}$, and then finally a differential distance $d\vec{r}$ further.

and

$$Q - K_0 = (x_k - \Gamma)\cos\theta_B - y_k \sin\theta_B \quad . \tag{21b}$$

Substituting these results into Eq. (14) gives the equation for the dispersion surfaces in orthogonal coordinates:

$$(x_k - \Gamma)^2 \cos\theta_B - y_k^2 \sin^2\theta_B = \nu^2 \quad , \tag{22}$$

where for convenience we have defined $\nu^2 \equiv \nu_G \nu_{-G}$. Strictly speaking ν^2 will be a complex number for an absorbing, noncentrosymmetric crystal. We will deal with this problem separately in discussing the effects of absorption in Sec. III E. Here, then, the symbol ν^2 is the real part of $\nu_G \nu_{-G}$.

The slope of the dispersion surface is then obtained by differentiating Eq. (22); we obtain

$$m_1 = \frac{dy_k}{dx_k} = \frac{(x_k - \Gamma)}{y_k} \cot^2\theta_B \quad . \tag{23}$$

The slope of a line normal to the dispersion surface is therefore

$$m_2 = -\frac{1}{m_1} = -\left(\frac{y_k}{x_k - \Gamma}\right) \tan^2\theta_B \quad . \tag{24}$$

A unit vector $\hat{j}$ along this line, which is the direction of the local neutron current, is therefore given by

$$\hat{j} = \frac{\hat{x} + m_2 \hat{y}}{(1 + m_2^2)^{1/2}}$$

$$= \frac{(x_k - \Gamma)\cos^2\theta_B \hat{x} - y_k \sin^2\theta_B \hat{y}}{[(x_k - \Gamma)^2 \cos^4\theta_B + y_k^2 \sin^4\theta_B]^{1/2}} \quad . \tag{25}$$

A unit vector $\hat{t}$ along the direction tangent to the dispersion surface is given by

$$\hat{t} = \frac{\hat{x} + m_1 \hat{y}}{(1 + m_1^2)^{1/2}} = \frac{m_2 \hat{x} - \hat{y}}{(1 + m_2^2)^{1/2}}$$

$$= \frac{(x_k - \Gamma)\cos^2\theta_B \hat{y} + y_k \sin^2\theta_B \hat{x}}{[y_k^2 \sin^4\theta_B + (x_k - \Gamma)^2 \cos^4\theta_B]^{1/2}} \quad . \tag{26}$$

In Eqs. (25) and (26), $\hat{x}$ and $\hat{y}$ are unit vectors along the x and y directions of Figs. 1 and 3. Note that the slope m_2 is the local slope dy/dx of the neutron trajectory in real space. It will be convenient to define a normalized slope

$$p \equiv \frac{m_2}{\tan\theta_B} = \frac{1}{\tan\theta_B} \frac{dy}{dx} \quad . \tag{27}$$

Using Eq. (24) we can calculate the rate of change of p with depth x into the crystal,

$$\frac{dp}{dx} = -\tan\theta_B \left[\frac{(dy_k/dx)}{x_k - \Gamma} - y_k \frac{(dx_k/dx) - (d\Gamma/dx)}{(x_k - \Gamma)^2} \right] \quad . \tag{28}$$

Using Eq. (24), the dispersion relation Eq. (22), and the definition of p [Eq. (27)], we can write

$$x_k - \Gamma = \pm \frac{\nu}{\cos\theta_B} (1 - p^2)^{-1/2} \tag{29}$$

and

$$y_k = \mp \frac{\nu}{\sin\theta_B} p (1 - p^2)^{-1/2} \quad . \tag{30}$$

In these equations, the upper sign applies to the β branch and the lower sign to the α branch. The derivatives on the right-hand side of Eq. (28) can also be expressed in terms of the normalized slope p using the differential geometry shown in Fig. 4, the expression for the unit vector $\hat{j}$ given by Eq. (25), and the definition of Γ [Eq. (20)]. We find that

$$\frac{dx_k}{dx} - \frac{d\Gamma}{dx} = -\frac{\tan\theta_B}{\cos\theta_B} \frac{m^2}{\hbar^2 k_0} \vec{g} \cdot \hat{y} p \tag{31}$$

and

$$\frac{dy_k}{dx} = \frac{m^2 \vec{g} \cdot \hat{y}}{\hbar^2 k_0 \cos\theta_B} \quad . \tag{32}$$

Substituting these results and the expressions (29) and (30) into Eq. (28), we have the differential for the trajectory which we have sought

$$\frac{dp}{dx} = \mp \tan\theta_B \frac{m^2 \vec{g} \cdot \hat{y}}{\hbar^2 k_0} \frac{1}{\nu} (1 - p^2)^{3/2} \quad . \tag{33}$$

The upper sign $(-)$ is for the β branch and the lower sign $(+)$ is for the α branch. Using the definition of p given by Eq. (27), this equation can be written as a second-order differential equation for the y coordinate of the trajectory as a function of x. We note that if the acceleration due to gravity $\vec{g}$ is perpendicular to the reciprocal-lattice vector $\vec{G} = G\hat{y}$, then the trajectories are straight lines, unaffected by gravity.

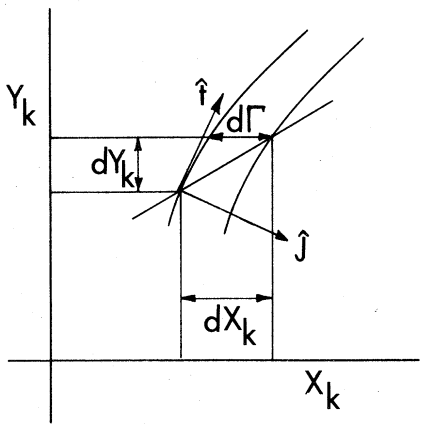

FIG. 4. Differential geometry used in deriving Eqs. (31) and (32).

The differential equation (33) is precisely of the same form as the one derived by Kato[11] for the trajectories of x rays in a strained perfect crystal. It will be convenient to define the parameter

$$\epsilon \equiv -2\sin\theta_B \frac{m^2 \vec{g}\cdot\hat{y}}{\hbar^2 k_0} \tag{34}$$

and to write Eq. (33) as

$$\nu \frac{d}{dx}\left(\frac{p}{(1-p^2)^{1/2}}\right) = \pm\frac{\epsilon}{2\cos\theta_B} \ . \tag{35}$$

This equation can easily be integrated to give the normalized slope p as a function of depth x,

$$\frac{p}{(1-p^2)^{1/2}} - \frac{p_0}{(1-p_0^2)^{1/2}} = \pm\frac{\epsilon}{2\nu\cos\theta_B}x \ . \tag{36}$$

The initial normalized slope of the trajectory at the entrance point A is denoted by p_0. Solving this equation for p and integrating again over x, we obtain the equation of the trajectory, which can be put in the form:

$$\frac{(y-y_c)^2}{\sin^2\theta_B} - \frac{(x-x_c)^2}{\cos^2\theta_B} = \left(\frac{2\nu}{\epsilon}\right)^2 \ , \tag{37}$$

which is the equation for a hyperbola.

There are two sets of coordinates (x_c,y_c) for the center of the hyperbola given by

$$x_c = \mp\frac{2\nu\cos\theta_B}{\epsilon}\frac{p_0}{(1-p_0^2)^{1/2}} \tag{38}$$

and

$$y_c = \mp\frac{2\nu\sin\theta_B}{\epsilon}\frac{1}{(1-p_0^2)^{1/2}} \ . \tag{39}$$

The upper signs refer to the β branch and the lower signs to the α branch.

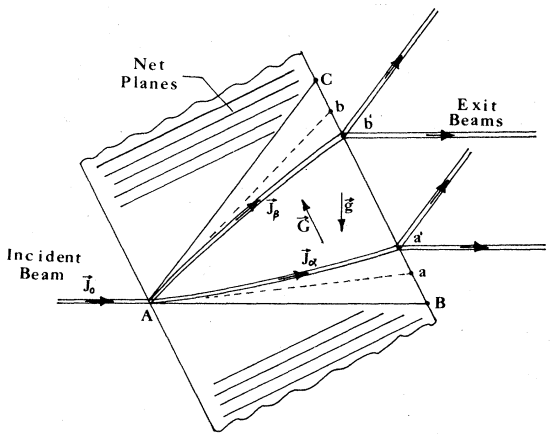

FIG. 5. Schematic diagram of typical hyperbolic neutron trajectories (under the influence of gravity) for the α and β branches of the dispersion surface.

In summary, the main result of this section has been to find that the trajectories of Bragg-reflecting neutrons inside a perfect crystal medium acted upon by Earth's gravitational field are hyperbolic. We schematically show typical trajectories for currents corresponding to the α and β branches in Fig. 5.

D. Wave amplitudes

We will now derive expressions for the wave amplitudes ψ_0 and ψ_G corresponding to each branch of the dispersion surface. The method used is similar to the one used by Kato[11] for the x-ray strain problem. The wave function for either branch is of the form

$$\psi = \psi_0 \exp(i\vec{K}_0\cdot\vec{r}) + \psi_G \exp(i\vec{K}_G\cdot\vec{r}) \ , \tag{40}$$

and the corresponding current density is calculated from the usual formula:

$$\vec{j} = \frac{\hbar}{2mi}(\psi^*\vec{\nabla}\psi + \psi\vec{\nabla}\psi^*) \ . \tag{41}$$

We find, then, that the local current density corresponding to a given branch is given by

$$\vec{j} = \frac{\hbar k_0}{m}(|\psi_0|^2\hat{s}_0 + |\psi_G|^2\hat{s}_G) \ , \tag{42}$$

where $\hat{s}_0$ and $\hat{s}_G$ are unit vectors along the incident wave vector $\vec{K}_0$ and the diffracted wave vector $\vec{K}_G$, respectively. We have again neglected terms involving the gradients of the wave amplitudes and wave vectors.

If the incident beam is of width w_0 and height h_0, the beam corresponding to a given branch will be of width w and height h_0 inside the crystal. This is shown in Fig. 6. The cross-sectional areas of the two beams are related by

$$\frac{a}{a_0} = \frac{w}{w_0} = \frac{\cos\theta}{\cos\theta_B} \ , \tag{43}$$

where θ is the angle which the initial current vector $\vec{j}$ makes with the x axis, that is $\cos\theta = \hat{x}\cdot\hat{j}$. Using Eq. (42), we can write an expression for $\vec{j}$, and we find that the total current flow associated with a given branch is

$$J = |\vec{j}|a = a_0\left(\frac{\hbar k_0}{m}\right)(|\psi_0|^2 + |\psi_G|^2) \ . \tag{44}$$

Aside from absorption, which we will discuss separately in the next section, this total current flow will be maintained along a given trajectory inside the crystal. However, the relative contributions from ψ_0 and ψ_G to this current flow will depend upon position $\vec{r}$. The ratio of the wave amplitudes at any point $\vec{r}$ for the branch $\gamma = \alpha$ or β is given by

$$C^\gamma(\vec{r}) = \frac{\psi_G^\gamma}{\psi_0^\gamma} = \frac{(Q-K_0^\gamma)}{\nu_{-G}} \ , \tag{45}$$

where we have used Eqs. (12a) and (16). We can express this ratio in terms of the local normalized slope of the trajectory using Eqs. (12b), (29), and (30). The result is

$$C^{\gamma}(\vec{r}) = \pm\left(\frac{\nu_G}{\nu_{-G}}\right)^{1/2}\left(\frac{1+p}{1-p}\right)^{1/2}, \quad \begin{cases} -\alpha \text{ branch} \\ +\beta \text{ branch} \end{cases} . \tag{46}$$

For continuity of the wave function across the entrant boundary, we require

$$\psi_0^{\alpha}(0) + \psi_0^{\beta}(0) = \Phi \tag{47a}$$

and

$$\psi_G^{\alpha}(0) + \psi_G^{\beta}(0) = 0 . \tag{47b}$$

For the symmetric Laue geometry, the initial tie points on the α and β branches will have equal, but opposite, normalized slopes, namely,

$$p_0^{\alpha} = -p_0^{\beta} . \tag{48}$$

Using Eqs. (46)–(48), we can express the initial values of the wave amplitudes in terms of the initial normalized slopes p_0^{γ} of the trajectories for each branch ($\gamma = \alpha$ or β) and the amplitude of the incident plane wave:

$$\psi_0^{\gamma}(0) = \tfrac{1}{2}(1 - p_0^{\gamma})\Phi \tag{49a}$$

and

$$\psi_G^{\gamma}(0) = \tfrac{1}{2}[(1-p_0^{\gamma})(1+p_0^{\gamma})]^{1/2}\left(\frac{\nu_G}{\nu_{-G}}\right)^{1/2}\Phi . \tag{49b}$$

Since the total current flow corresponding to a given branch is independent of $\vec{r}$, we must have

$$|\psi_0^{\gamma}(\vec{r})|^2 + |\psi_G^{\gamma}(\vec{r})|^2 = |\psi_0^{\gamma}(0)|^2 + |\psi_G^{\gamma}(0)|^2 . \tag{50}$$

Using Eq. (46) again, we find

$$|\psi_0^{\gamma}|^2 = \tfrac{1}{4}(1-p_0^{\gamma})(1-p^{\gamma})|\Phi|^2 \tag{51}$$

and

$$|\psi_G^{\gamma}|^2 = \tfrac{1}{4}(1-p_0^{\gamma})(1+p^{\gamma})|\Phi|^2 . \tag{52}$$

We have taken ν_G/ν_{-G} to be equal to 1. From Eq. (36) we can express the normalized slope p at a given depth x in the crystal in terms of the initial normalized slope p_0, the result is

$$p^{\gamma}(x) = \frac{\pm\epsilon/(2\cos\theta_B)x + p_0^{\gamma}[1-(p_0^{\gamma})^2]^{-1/2}}{(1+\{\pm\epsilon/(2\cos\theta_B)x + p_0^{\gamma}[1-(p_0^{\gamma})^2]^{-1/2}\}^2)^{1/2}} . \tag{53}$$

Thus, given an initial tie point, which is specified by p_0^{γ} we have explicit expressions for the wave amplitudes at any point along the trajectories. The angular deviaton $\Delta\theta$ of the incident ray from the exact Bragg condition corresponding to p_0^{γ} can be found from Eq. (30) and the geometry of Fig. 2,

$$\Delta\theta = \frac{\mp 2\nu}{k_0 \sin 2\theta_B}\frac{p_0^{\gamma}}{(1-p_0^{\gamma 2})^{1/2}} . \tag{54}$$

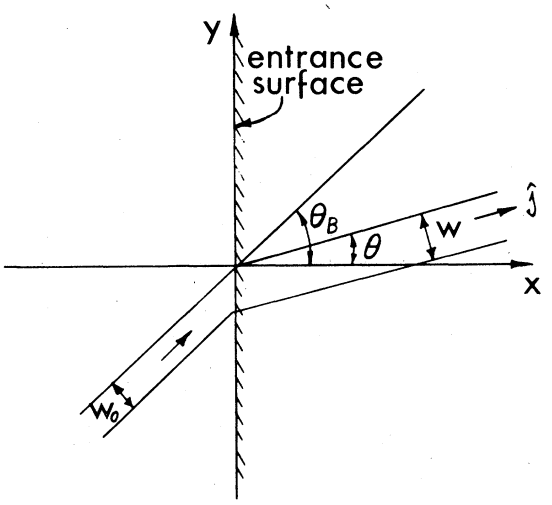

FIG. 6. This diagram shows the change in the beam cross-sectional area at the entrant surface of the crystal.

E. Absorption

The total current flow along a given trajectory will be attenuated due to absorption. Because the absorption coefficient depends upon the tie point and the tie point migrates with position $\vec{r}$ along the trajectory, the calculation of the absorption factor A_{γ} appropriate to a given branch $\gamma(=\alpha$ or $\beta)$ will depend upon p_0^{γ} and x. The current at a given position $\vec{r}$ will be related to the current $J(0)$ at the entrant surface by

$$J_{\gamma}(r) = A_{\gamma}J_{\gamma}(0) . \tag{55}$$

The absorption factor is given by

$$A = \exp\left(-\int \mu_j\, ds\right) , \tag{56}$$

where μ_j is the probability for absorption per unit path length along the trajectory (linear absorption coefficient); that is, along the vector $\vec{j}$. An expression for μ_j in terms of the normalized slope of the trajectory is derived in the Appendix [Eq. (A16)]. A differential line element along the trajectory is

$$ds = dx(1+p^2\tan\theta_B)^{1/2} . \tag{57}$$

Thus, using Eq. (A16) we have

$$A = \exp\left(-\frac{\mu_0}{\cos_B}\int_0^T [1 \mp C_0(1-p^2)^{1/2}]\, dx\right) . \tag{58}$$

The constant C_0 is defined by Eq. (A19), μ_0 is the isotropic absorption coefficient, and T is the crystal thickness. Using Eq. (53), we can in fact carry out the integration. The result is

$$A_\gamma = \exp\left\{-\frac{\mu_0 T}{\cos\theta_B}\left[1 \mp \alpha^{-1} C_0 \ln\left[\frac{\alpha + a + [(\alpha+a)^2+1]^{1/2}}{a+(a^2+1)^{1/2}}\right]\right]\right\} , \tag{59}$$

where we have defined

$$\alpha = \pm \frac{\epsilon T}{2\cos\theta_B \mathrm{Re}(\nu)} \tag{60}$$

and

$$a = \frac{p_0^\gamma}{(1-p_0^{\gamma 2})^{1/2}} = \mp \frac{k_0 \sin 2\theta_B}{2\,\mathrm{Re}(\nu)} \Delta\theta \ . \tag{61}$$

We have used Eq. (54) to relate the initial normalized slope p_0^γ to the angular deviation $\Delta\theta$ of the incident ray from the exact Bragg condition. In using the results of Secs. C and D we have made the replacement $\nu \rightarrow \mathrm{Re}(\nu)$. In Eqs. (59) and (60) the upper signs refer to the β branch and the lower signs to the α branch.

F. Numerical calculations

If we limit ourselves to considering centrosymmetric crystals, the diffracted intensity corresponding to a given branch can be written in closed form. The result is dependent upon the scaled angular variable a [Eq. (61)] the parameter α [Eq. (60)], and the linear coefficient of absorption. Using Eqs. (52), (53), and (59) we have

$$I_G^\gamma = \exp\left\{-\frac{\mu_0 T}{\cos\theta_B}\left[1 \pm \alpha^{-1} \ln\left[\frac{\alpha + a + [(\alpha+a)^2+1]^{1/2}}{a+(a^2+1)^{1/2}}\right]\right]\right\}\left[1 - \frac{a}{(1+a^2)^{1/2}}\right]\left[1 - \frac{\alpha+a}{[1+(\alpha+a)^2]^{1/2}}\right] . \tag{62}$$

A plot of this function versus the scaled angular variable a is the rocking curve expected for a plane monochromatic incident beam. For the case of zero absorption ($\mu_0 = 0$) a series of rocking curves is shown in Fig. 7. The curves displayed are for the β branch. We note two interesting effects resulting from gravity: The first is that the sense of the gravitational field (parallel to $\vec{G}$ or antiparallel to $\vec{G}$) is important. When $\hat{g}\cdot\hat{G}(=\hat{g}\cdot\hat{y})$ is positive, α is positive for the β branch, and increasing this dot product increases the diffracted intensity corresponding to the β branch. However, for $\hat{g}\cdot\hat{G}$ negative, the intensity decreases with α increasing negatively. Precisely the opposite effects occur for the α-branch intensity. The second observation is that gravity substantially affects the width and centroid of the rocking curves. The integrated intensity corresponding to a given branch is

$$g^\gamma\left(\alpha, \frac{\mu_0 T}{\cos\theta_B}\right) = \int_{-\infty}^{\infty} I_G^\gamma \, da \ . \tag{63}$$

In the case of zero absorption, and zero gravity, this integral can be evaluated easily. The result is

$$g_G^\gamma(0,0) = \tfrac{1}{4}\pi \ . \tag{64}$$

We show in Fig. 8 the results of a numerical calculation of integrated intensity corresponding to each branch as a function of gravity as expressed through the parameter α. We see that for positive increasing α, g^β increases while g^α decreases. For negative α the reverse is true. The sum $g^\alpha + g^\beta$ increases with increasing $|\alpha|$ and is symmetric about $\alpha = 0$. These

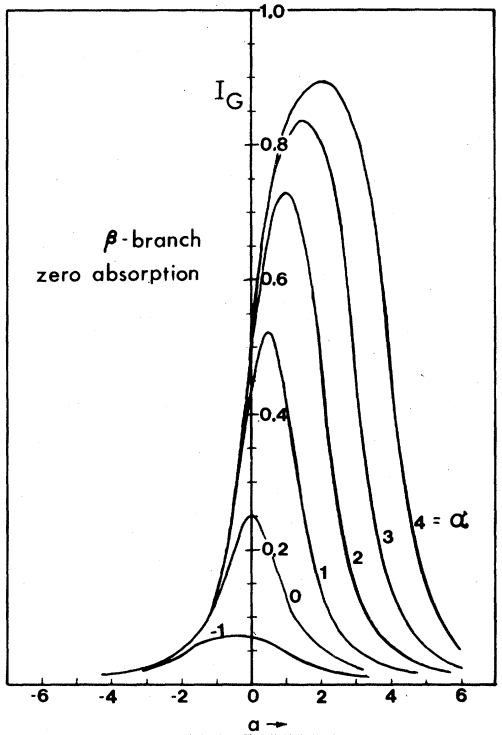

FIG. 7. Rocking curves for the β-branch diffracted intensity for various strengths of the gravitational field. The parameter α is proportional to the acceleration due to gravity ($\vec{g}$); it is defined by Eqs. (34) and (60). The parameter a is defined by Eq. (61) and is proportional to the angular deviation $\Delta\theta$ of the incident ray from the exact Bragg condition. This parameter is the same as the parameter y in Zachariasen's book (see Ref. 2).

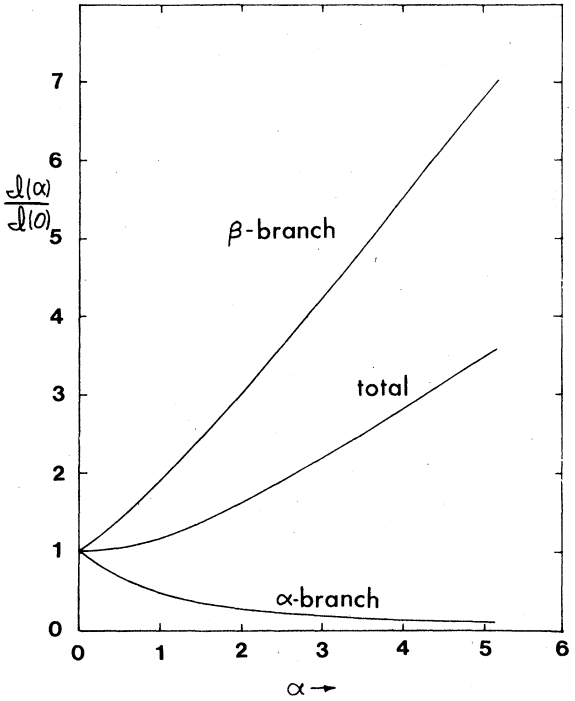

FIG. 8. This figure shows the effect of increasing gravity [as expressed through the parameter α Eq. (60)] on the integrated intensity of the α branch $[\mathcal{g}^{\alpha}(\alpha)/\mathcal{g}^{\alpha}(0)]$, the β branch $[\mathcal{g}^{\beta}(\alpha)/\mathcal{g}^{\beta}(0)]$, and on the sum of the integrated intensities for the α and β branches $\mathcal{g}(\alpha)/\mathcal{g}(0) = [\mathcal{g}^{\alpha}(\alpha)+\mathcal{g}^{\beta}(\alpha)]/[\mathcal{g}^{\alpha}(0)+\mathcal{g}^{\beta}(0)]$. This figure is drawn for zero absorption ($\mu_0=0$).

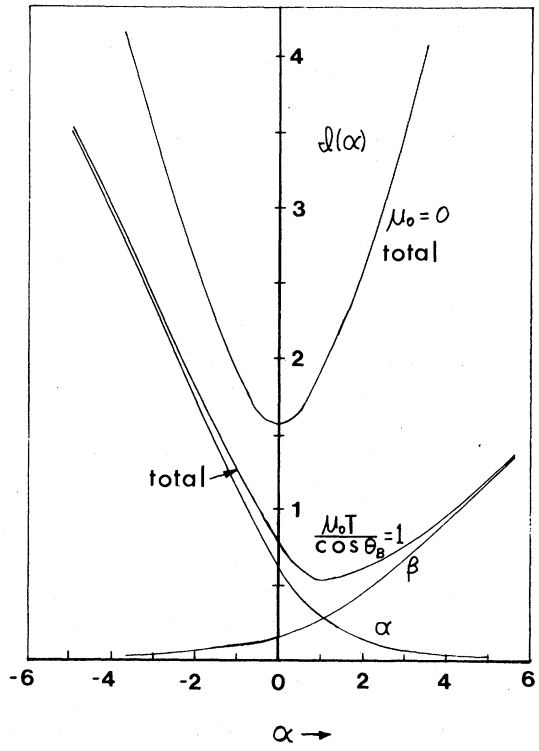

FIG. 9. This figure shows the influence of gravity on the total integrated intensity for values of absorption $\mu_0 T/\cos\theta_B = 0$ and 1.

results are identical to the results of Kato[11] for the strain problem as shown in his Fig. 5 if we identify our parameter α with his parameter $\sqrt{A}$.

These results can be qualitatively understood simply on the basis of the migration of the tie points resulting from the influence of gravity which in turn effects the wave amplitude ratios $\psi_G^{\gamma}/\psi_0^{\gamma}$. However, a qualitative understanding becomes more difficult with the addition of absorption. We show in Fig. 9 results of numerical calculations of the integrated intensity for the case when $\mu_0 T/\cos\theta_B = 1.0$. We see that the total integrated reflectivity $(\mathcal{g}^{\alpha}+\mathcal{g}^{\beta})$ is no longer symmetric in the parameter α. Increasing α from $\alpha=0$ initially decreases the reflectivity; however, at $\alpha \approx 1$, the integrated reflectivity begins to increase again. For negative α, the integrated reflectivity increases rapidly with $|\alpha|$.

The effect of gravity on the integrated reflectivity, for other values of $\mu_0 T/\cos\theta_B$ is shown in Fig. 10. The behavior is clearly complicated. These results support our original intuition that it is even difficult to predict the sign of the effect of gravity on the reflectivity.

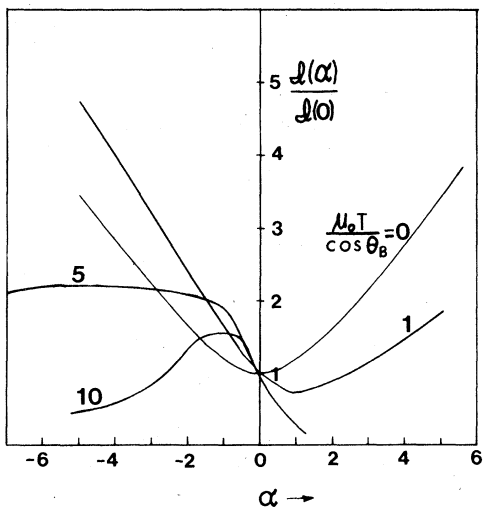

FIG. 10. The figure shows the relative change in integrated intensity due to gravity for various values of absorption. $U = \mu_0 T/\cos\theta_B$.

IV. COUPLED-PARTIAL-DIFFERENTIAL-EQUATION METHOD

In the last section we did not consider the effects of interference between the α- and β-branch wave functions which leads to the Pendellösung fringe structure. In order to include this interference term we must evaluate the phase integral for each branch:

$$\phi = \int \vec{K}_0^{\gamma} \cdot d\vec{r} \ , \tag{65}$$

where ϕ is the phase, and the integral is taken along the trajectory. This integration can in fact be carried out as has been demonstrated by Kato in his work on the x-ray strain problem.[11] However, there is an alternative approach which incorporates the Pendellösung interference structure in a natural way. It is directly analogous to the methods first described by Takagi[13] and Taupin[14] to analyze the effects of strain on the dynamical diffraction of x rays.

A. Basic equations

We begin with the wave equation (6) and again assume that the solution is a Bloch function

$$\psi(\vec{r}) = \sum_{\vec{G}} \psi_{\vec{G}}(\vec{r}) \exp(i\vec{K}_0 \cdot \vec{r} + i\vec{G} \cdot \vec{r}) \ . \tag{66}$$

However, here we fix the value of the internal wave vector $\vec{K}_0$ at the index-of-refraction-corrected value of the external incident wave vector, that is

$$\vec{K}_0 = \vec{K} = \left(k_0 - \frac{1}{2} \frac{v_0}{k_0} \right) \hat{S}_0 \ . \tag{67}$$

The unit vector $\hat{S}_0$ is along the incident beam direction as shown in Fig. 1. A unit vector along the diffracted-beam direction is $\hat{S}_G$ as shown in Fig. 1. Thus, the spatial dependence of ψ resulting from the spatial dependence of $\vec{K}_0$ in the eikonal approach is now incorporated into the wave amplitudes $\psi_G(\vec{r})$. In substituting Eq. (66) into the wave equation (6), we will therefore need to keep terms involving the gradient of the wave amplitudes. However, we neglect terms involving $\nabla^2 \psi_{\vec{G}}$ which can be shown to be numerically small compared to $\vec{K} \cdot \vec{\nabla} \psi_{\vec{G}}$.

Within the scope of this approximation, we find that the wave equation requires

$$\psi_{\vec{G}'}[k_0^2 - (m^2 \vec{g} \cdot \vec{r}/\hbar^2) - (\vec{K} + \vec{G}')^2] + 2i(\vec{K} + \vec{G}') \cdot \vec{\nabla} \psi_{\vec{G}'} = \sum_{\vec{G}''} v_{\vec{G}' - \vec{G}''} \psi_{\vec{G}''} \ . \tag{68}$$

We again assume that the incident wave vector $\vec{k}_0$ is oriented close to the Bragg condition for only one particular reciprocal-lattice vector $\vec{G}$. Thus, only two wave amplitudes ψ_0 and ψ_G will be large, and the above infinite set of coupled equations reduces to the following pair of coupled differential equations:

$$(Q^2 - K^2)\psi_0 + 2i\vec{K} \cdot \vec{\nabla} \psi_0 - v_{-\vec{G}} \psi_{\vec{G}} = 0 \tag{69a}$$

and

$$-v_{\vec{G}} \psi_0 + 2i\vec{K}_{\vec{G}} \cdot \vec{\nabla} \psi_{\vec{G}} + (Q^2 - K_{\vec{G}}^2)\psi_{\vec{G}} = 0 \ , \tag{69b}$$

where Q is defined by Eq. (13). In these equations

$$\vec{K} = K\hat{S}_0$$

and

$$\vec{K}_{\vec{G}} = \vec{K} + \vec{G} = K\hat{S}_G \ . \tag{70}$$

Thus, if we make the approximation

$$Q + K = Q + K_{\vec{G}} \approx 2K \approx 2k_0 \ , \tag{71}$$

we can write Eqs. (69) in the form

$$(Q - K)\psi_0 - \frac{v_{-\vec{G}}}{2K} \psi_{\vec{G}} = -i \frac{\partial \psi_0}{\partial S_0} \tag{72}$$

and

$$-\frac{v_{\vec{G}}}{2K} \psi_0 + (Q - K)\psi_{\vec{G}} = -i \frac{\partial \psi_{\vec{G}}}{\partial S_G} \ . \tag{73}$$

The position of a given point $\vec{r}$ inside the crystal is given in terms of the nonorthogonal coordinates (S_0, S_G) shown in Fig. 1. These equations can be put in simpler form by writing

$$\psi_0 = e^{i\theta_0} U_0 \tag{74}$$

and

$$\psi_{\vec{G}} = e^{-i\theta_G} U_G \ , \tag{74}$$

where

$$\theta_0 = [\hat{g} \cdot \hat{S}_0 \tfrac{1}{2} S_0^2 + \hat{g} \cdot \hat{S}_G (\tfrac{1}{2} S_G^2 + S_0 S_G)] \frac{m^2 g}{\hbar^2 k_0} \tag{75a}$$

and

$$\theta_G = [\hat{g} \cdot \hat{S}_G \tfrac{1}{2} S_G^2 + \hat{g} \cdot \hat{S}_0 (\tfrac{1}{2} S_0^2 + S_0 S_G)] \frac{m^2 g}{\hbar^2 k_0} \ . \tag{75b}$$

Substitution of Eqs. (74) into (72) and (73) gives

$$v_{-G} U_G \exp(i\epsilon S_0 S_G) = i \frac{\partial U_0}{\partial S_0} \tag{76}$$

and

$$v_G U_0 \exp(-i\epsilon S_0 S_G) = i \frac{\partial U_G}{\partial S_G} \ , \tag{77}$$

where ϵ is defined by Eq. (34) and v_G is given by Eq. (15). These equations are precisely of the same form as the Takagi-Taupin equations as written down by Katagawa and Kato.[15] We identify our parameter ϵ with their strain parameter f:

$$f = \frac{\partial^2}{\partial S_0 \partial S_G} (\vec{G} \cdot \vec{U}) \ , \tag{78}$$

where $\vec{U}(r)$ is the atomic displacement field resulting from strain.

B. δ-function incident beam

We consider now the problem where the incident beam is a plane wave [Eq. (18)] with a slit of infinitesimal width placed in front of the crystal at point A as shown in Fig. 1. This slit will diffract the incident beam, such that over the angular acceptance range of the crystal, the beam incident on the crystal will appear to be a monochromatic spherical wave. There are a number of mathematical techniques that can be used to solve Eqs. (76) and (77) for this geometry. The technique used by Katagawa and Kato was to solve these coupled partial differential equations directly using Laplace-transform methods. An alternative technique is to write these equations in integral form and then solve the resulting integral equations. We find this method easy to apply in this case. For a distributed incident beam (finite-width entrant slit) it is probably easier to utilize power-series-expansion techniques or Riemann-function techniques.

Integrating Eq. (76) from 0^- to S_0, we have

$$i[U_0(S_0,S_G)-U_0(0^-,S_G)] = \int_{0^-}^{S_0} \nu_{-G} U_G(S_0',S_G)\exp(i\epsilon S_0' S_G)\,dS_0' \quad ; \tag{79}$$

and integrating Eq. (77) from 0^- to S_G, we have

$$i[U_G(S_0,S_G)-U_G(S_0,0^-)] = \int_{0^-}^{S_G} \nu_G U_0(S_0,S_G')\exp(-i\epsilon S_0 S_G')\,dS_G' \quad . \tag{80}$$

The symbol "0^-" means infinitesimally negative. For a δ-function incident beam, we have the boundary conditions

$$U_G(S_0,0^-)=0 \tag{81}$$

and

$$U_0(0^-,S_G)=\Phi\delta(S_G) \quad , \tag{82}$$

where $\delta(S_G)$ is a Dirac δ function. Substituting U_0 from Eq. (79) into Eq. (80) and using the boundary conditions Eqs. (81) and (82), we have an integral equation for $U_G(S_0,S_G)$:

$$U_G(S_0,S_G)=\nu_G\Phi-\nu^2\int_{0^-}^{S_G} dS_G'\int_{0^-}^{S_0} dS_0'\exp[i\epsilon S_G'(S_0'-S_0)]U_G(S_0',S_G') \quad . \tag{83}$$

Define $W_G(q,S_G)$ as the Laplace transform of $U_G(S_0,S_G)$; that is

$$W_G(q,S_G)=\int_{0^-}^{\infty} U_G(S_0,S_G)e^{-qS_0}\,dS_0 \quad , \tag{84}$$

where q is the Laplace-transform variable. Using this definition and the standard rules for the Laplace transform of a convolution integral we obtain from Eq. (83) the linear integral equation for $W_G(q,S_G)$

$$W_G(q,S_G)=\frac{\nu_G\Phi}{q}-\nu^2\int_{0^-}^{S_G} dS_G'\frac{1}{q+i\epsilon S_G'}W_G(q,S_G') \quad . \tag{85}$$

This equation is of the Fredholm type, and the solution can be written as a Born series, namely,

$$W_G(q,S_G)=(1-\nu^2L+\nu^4L^2-\cdots\nu^{2n}L^n\cdots)\frac{\nu_G\Phi}{q} \quad , \tag{86}$$

where the operator L is defined by

$$Lf=\int_0^{S_G} dS_G'\frac{f(q,S_G')}{q+i\epsilon S_G'} \tag{87}$$

and L^n means to apply this operator n times to the function f. If we let

$$x=\ln\left(1+\frac{i\epsilon}{q}S_G\right) \quad , \tag{88}$$

then this operator takes the simple form

$$Lf=-\frac{i}{\epsilon}\int_0^x dx' f(q,x') \quad . \tag{89}$$

Since $\nu_G\Phi/q$ is a constant (independent of the variable of integration), application of the operator $(1-\nu^2L+\nu^4L^2-\cdots\nu^{2n}L^n)$ in Eq. (86) gives a simple power series

$$W_G(q,S_G)=\frac{\nu_G\Phi}{q}\sum_{n=0}^{\infty}(-)^n\nu^{2n}\frac{1}{(i\epsilon)^n}\frac{x^n}{n!}=\frac{\nu\Phi}{q}e^z \quad , \tag{90}$$

where

$$z=\frac{i\nu^2}{\epsilon}\ln\left(1+\frac{i\epsilon S_G}{q}\right) \quad . \tag{91}$$

If we define

$$\beta=\frac{i\nu^2}{\epsilon} \quad , \tag{92}$$

then W_G can be written as

$$W_G(q,S_G)=\frac{\nu_G\Phi}{q}\left(1+\frac{iS_G}{q}\right)^{\beta} \quad . \tag{93}$$

Using the binomial theorem, this can be rewritten as

$$W_G(q,S_G)=\frac{\nu_G\Phi}{q}\sum_{n=0}^{\infty}(\beta)_n\frac{1}{q^n n!}(i\epsilon S_G)^n \quad , \tag{94}$$

where $(\beta)_n$ is the Pochammer symbol

$$(\beta)_n=\beta(\beta+1)(\beta+2)\cdots(\beta+n-1);\quad (\beta)_0=1 \quad . \tag{95}$$

The inverse Laplace transform of Eq. (94) can easily be calculated using the rule

$$\mathcal{L}^{-1}\left[\frac{1}{q^{m+1}}\right]=\frac{S_G^m}{m!} \quad . \tag{96}$$

Finally, then we have the diffracted wave amplitude

$$U_G(S_0,S_G)=\nu_G\Phi\sum_{n=0}^{\infty}(\beta)_n\frac{1}{(n!)^2}(i\epsilon S_0S_G)^n$$

$$=\nu_G\Phi M(\beta,1,i\epsilon S_0S_G) \quad . \tag{97}$$

The function. M is Kummer's hypogeometric function.[16] This formula agrees with Katagawa and Kato's results aside from an unimportant multiplicative phase factor (i).

C. Small ϵ/ν^2

In the limit when the gravitation potential is small compared to the crystal potential, that is, ϵ/ν^2 is small, it is easy to show that

$$(\beta)_n(i\epsilon)^n=(-)^n\nu^{2n}\left[1-\tfrac{1}{2}(n-1)n\frac{i\epsilon}{\nu^2}+\cdots\right] \quad . \tag{98}$$

Substituting this into Eq. (97), we have approximately

$$U_G(S_0,S_G)\approx\nu_G\Phi\left[\sum_{n=0}^{\infty}(-)^n\frac{[2\nu(S_0S_G)^{1/2}]^{2n}}{2^{2n}n!n!}-i\frac{\epsilon}{\nu^2}\sum_{n=0}^{\infty}(-)^n\frac{n(n-1)}{2^{2n+1}n!n!}[2\nu(S_0S_G)^{1/2}]^{2n}\right]$$

$$=\nu_G\Phi[J_0(2\nu(S_0S_G)^{1/2})-\tfrac{1}{2}i\epsilon S_0S_GJ_2(2\nu(S_0S_G)^{1/2})] \quad , \tag{99}$$

where J_n are the ordinary Bessel function of the first kind. Thus, in the absence of gravitational effects ($\epsilon=0$), we see that the diffracted intensity is given by

$$I_G=|\nu_G|^2|\Phi|^2J_0^2(2\nu(S_0S_G)^{1/2}) \tag{100}$$

for the case of zero absorption. This result agrees with Kato's original result[17] for the dynamical diffraction of a spherical incident wave.

D. Intensity distribution along the exit surface

We will now confine our attention to the symmetrical Laue case for a crystal of thickness T. Along the exit surface

$$S_0=\frac{1}{2}\left(\frac{T}{\cos\theta_B}+\frac{y}{\sin\theta_B}\right) \tag{101}$$

and

$$S_G=\frac{1}{2}\left(\frac{T}{\cos\theta_B}-\frac{y}{\sin\theta_B}\right) \quad . \tag{102}$$

The variable which occurs in the result Eq. (97) is the product S_0S_G. We can write this in terms of a variable p, similar to the variable used in the eikonal theory; we get

$$S_0S_G=\left(\frac{T}{2\cos\theta_B}\right)^2(1-p^2) \quad , \tag{103}$$

where

$$p\equiv\frac{y/T}{\tan\theta_B} \quad . \tag{104}$$

Thus p ranges from -1 to $+1$ across the Borrmann fan. The total diffracted intensity at a given value of p is given by

$$I_G=|\nu_G|^2|\Phi|^2|M|^2\exp(-\mu_0T/\cos\theta_B) \quad , \tag{105}$$

where M is given by Eq. (97), and the absorption factor $\exp(-\mu_0T/\cos\theta_B)$ enters here because the wave vector $\vec{K}$ in Eq. (67) will have an imaginary part due to the fact that v_0 will be complex for an absorbing crystal. For an explanation of the origin of the $1/\cos\theta_B$ in the exponent see the Appendix. Since M depends upon the variable S_0S_G as given by Eq. (103), a plot of I_G vs p will be symmetric about $p=0$ (or $y=0$). The intensity distribution across the Borrmann fan on the exit surface depends on three dimensionless parameters

$$X_1=\mathrm{Re}\left(\frac{\nu T}{\cos\theta_B}\right) \quad , \tag{106}$$

$$X_2=\mathrm{Im}\left(\frac{\nu T}{\cos\theta_B}\right) \quad , \tag{107}$$

and

$$X_3=\frac{\epsilon T^2}{\cos^2\theta_B} \quad . \tag{108}$$

Thus the parameter α defined in Sec. III [Eq. (60)] is

$$\alpha=\frac{X_3}{2X_1} \quad . \tag{109}$$

The parameter X_1 is proportional to the neutron-nuclear interaction potential, X_2 is proportional to the

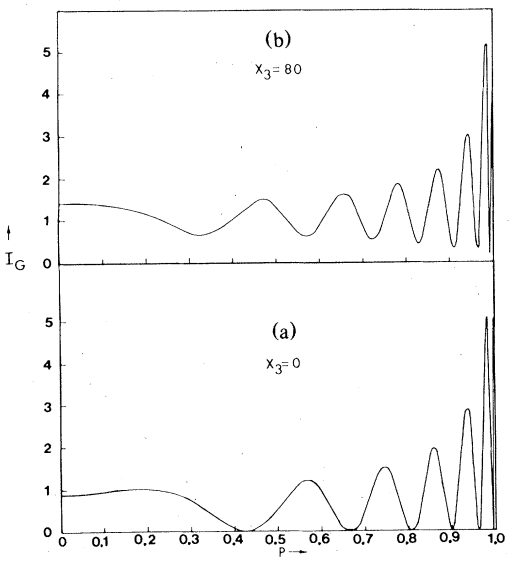

FIG. 11. (a),(b) Diffracted-beam profile across the Borrmann triangle on the exit surface (between points B and C in Fig. 1). The parameter $X_2=0$ for the drawing, which means zero absorption. The parameter $X_1=20$; it is proportional to the neutron-nuclear interaction potential [see Eq. (106)]. The parameter X_3 is proportional to the acceleration g due to gravity [see Eq. (108)]. We see that gravity increases the diffracted intensity, but reduces the Pendellösung fringe contrast.

linear absorption coefficient, and X_3 is proportional to the gravitational potential. For a centrosymmetric Bravais lattice

$$X_2 = -\frac{\mu_0 T}{2\cos\theta_B} \quad . \tag{110}$$

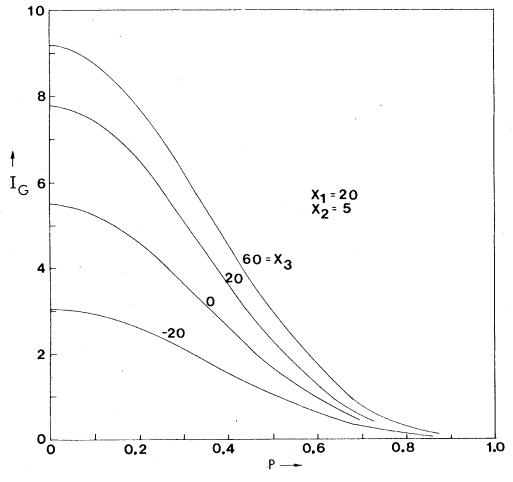

FIG. 12. Diffracted-beam profiles for a case of strong absorption $X_2=5$. Here $X_1=20$. We see that when $\hat{g}\cdot\hat{y}$ is negative, the intensity increases; while when $\vec{g}\cdot\vec{y}$ is positive, the intensity decreases due to gravity.

The effect of the gravitational potential on the diffracted intensity profile is shown in Fig. 11 in the case of zero absorption ($X_2=0$) with $X_1=20$. In part (a) of this figure the $X_3=0$ (no gravity), while in part (b) the parameter $X_3=80$ (which corresponds to $\alpha = X_3/2X_1 = 2$). We see that the effect of gravity is to reduce the contrast in the Pendellösung interference structure and to substantially shift the positions of the minima. Increasing the absorption tends to wash out the Pendellösung interference structure and make the effects of gravity much more important. These effects are shown in Fig. 12.

E. Integrated intensity

The integrated intensity is obtained by integrating the diffracted intensity I_G across the exit surface from point B to point C (Fig. 1). This is equivalent to integrating over the variable p. To place this integrated intensity on the same scale as in Sec. III, it should be written as

$$\mathcal{I}_G = \left|\frac{\nu_G T}{\cos\theta_B}\right| \int_{-1}^{+1} |M|^2 \, dp \quad . \tag{111}$$

The effect of gravity (as expressed through the parameter X_3) on the integrated intensity is shown in Fig. 13 for various values of absorption (as expressed through the parameter X_2). We again see that the effects of gravity are much more important for an absorping crystal. These results are in agreement with the numerical calculations of the integrated intensity given in Sec. III when presented in the normalized fashion shown in Fig. 13.

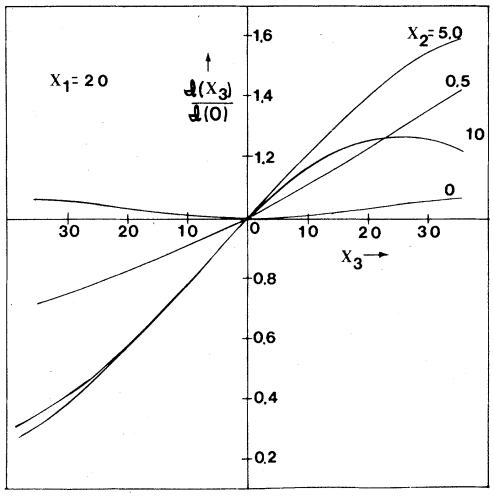

FIG. 13. Relative change in integrated intensity resulting from gravity (X_3) for various values of the absorption parameter (X_2). Here $X_1=20$. This figure is the result of numerical (computer) calculations based on the coupled-partial-differential-equation method.

TABLE I. (222) reflection in InSb. Wavelength $\lambda = 2.5$ Å. Absorption cross section $\sigma_a = 266$ b. Absorption coefficient $\mu_0 = 3.97\ \text{cm}^{-1}$. Lattice parameter = 6.45 Å. Bragg angle $\theta_B = 42.17°$. Scattering lengths: $b_{\text{In}} = (0.39 + 0.0123i) \times 10^{-12}$ cm, $b_{\text{Sb}} = 0.56 \times 10^{-12}$ cm. Structure factor $F_{222} = 4(b_{\text{In}} - b_{\text{Sb}}) = (-0.68 + 0.0492i) \times 10^{-12}$ cm. $\text{Re}(\nu) = \text{Re}(\nu_{222}) = -63.4\ \text{cm}^{-1}$. $\text{Im}(\nu) = \text{Im}(\nu_{222}) = 4.59\ \text{cm}^{-1}$. $m^2 g/\hbar^2 k_0 = 9.837\ \text{cm}^{-2}$, $g = 980\ \text{cm s}^{-2}$.

Crystal thickness T (cm)	$\hat{g}\cdot\hat{y}$	ϵ (cm^{-2})	α	$\frac{\mu_0 T}{\cos\theta_B}$	X_1	X_2	X_3	$\frac{\mathcal{I}(\alpha)}{\mathcal{I}(0)}$
1.0	+1	−13.21	∓0.141	5.36	−85.5	6.19	−24.05	1.128
2.0	+1	−13.21	∓0.282	10.72	−171.1	12.38	−96.18	1.233
5.0	+1	−13.21	∓0.705	26.8	−427.7	30.97	−601.1	0.982
1.0	−1	+13.21	±0.141	5.36	−85.5	6.19	24.05	0.875
2.0	−1	+13.21	±0.282	10.72	−171.1	12.38	96.18	0.722
5.0	−1	+13.21	±0.705	26.8	−427.7	30.97	601.1	0.254

V. DISCUSSION AND CONCLUSIONS

In the partial-differential-equation method of solution, the concept of the α and β branches of a dispersion does not arise. It therefore appears that the eikonal approach has no direct connection with this method, even though the fundamental equation in both cases is the Schrödinger equation. This connection has in fact been made in the paper by Katagawa and Kato[15] in which they show that the inverse Laplace-transform integral of Eq. (90), when evaluated by the method of steepest descents, gives precisely the eikonal solutions in which the branch structure is recovered.

We have carried out a number of specific numerical calculations on the expected magnitudes of the effect of gravity and a magnetic-field gradient on the dynamical diffraction of neutrons from various crystals. We are planning to carry out various experiments using Gd garnate, Si, CdS, InSb, and quartz. As an example, we display results in Table I for the integrated intensity for the (222) reflection in InSb in the symmetric Laue geometry for various crystal thicknesses. The predicted effects are large. The magnitude of the effect is dependent upon the ratio of the acceleration due to gravity ($\vec{g}$) to the neutron-nuclear potential.

One, of course, has no direct control on the magnitude of $\vec{g}$. However, as we mentioned in the Introduction, a magnetic field gradient of 170 G/cm creates an acceleration of a polarized neutron equivalent to $g = 980\ \text{cm/s}^2$. A field gradient of 10 times this magnitude is easy to achieve. Under such conditions very large effects on the profile of the diffracted beam and on the integrated intensity are predicted to occur. An interesting experiment has recently been carried out by Zeilinger and Shull[18] in which they have observed the effect of the Zeeman splitting in a uniform magnetic field on the dynamical diffraction of neutrons in Si. The small shifts in wave vector resulting from the magnetic field results in significant intensity differences.

In conclusion, it should be pointed out that essentially no systematic experimental work has been carried out on the effects of strain in the dynamical diffraction of neutrons. There is a large theoretical and experimental literature on the effects of strain in x-ray diffraction. We have shown in this paper the intimate connection between the effects of gravitational and magnetic fields on the dynamical diffraction of neutrons with the effects of strain on the dynamical diffraction of x rays. Future work in this area will certainly benefit by this connection.

ACKNOWLEDGMENTS

I have benefited greatly from many useful discussions with Roberto Colella (Purdue University), G. W. Ford (University of Michigan), U. Bonse (Dortmund, Germany), and A. Zeilinger (Vienna, Austria). This work has been supported by the National Science Foundation's Atomic, Molecular, and Plasma Physics Program through Grant No. 76 08960.

APPENDIX: ABSORPTION COEFFICIENT μ_j

For an absorbing crystal, the neutron-nuclear scattering lengths b_n are complex. Therefore the structure factors

$$F_{\vec{G}} = \sum_n b_n \exp(i\vec{G}\cdot\vec{r}_n) \tag{A1}$$

and the Fourier components of the potential

$$v_{\vec{G}} = 4F_{\vec{G}}/V_{\text{cell}} \tag{A2}$$

will also be complex. The internal wave vector $\vec{K}_0$ must therefore have an imaginary part; we write it as

$$\vec{K}_0 = \vec{K}_0' + i\vec{K}_0'' \ . \tag{A3}$$

In order to satisfy the boundary conditions at the entrant surface to the crystal, the imaginary part of $\vec{K}_0$ must be normal to the surface. In general, K_0''/K_0' will be very small, even for strongly absorbing materials, thus

$$K_0 = (K_0'^2 - K_0''^2 + 2i\vec{K}_0' \cdot \vec{K}_0'')^{1/2}$$
$$\approx K_0' + iK_0'' \cos\theta_B \ . \tag{A4}$$

If we define

$$\xi_0 = Q - K_0 = \xi_0' + i\xi_0'' \tag{A5}$$

and

$$\xi_G = Q - K_G = \xi_G' + i\xi_G'' \ , \tag{A6}$$

the dispersion relation Eq. (14) takes the form

$$\xi_0'\xi_G' - \xi_0''\xi_G'' = \mathrm{Re}(\nu^2) \tag{A7}$$

and

$$\xi_0'\xi_G'' + \xi_G'\xi_0'' = \mathrm{Im}(\nu^2) \ . \tag{A8}$$

$\mathrm{Re}(\nu^2)$ and $\mathrm{Im}(\nu^2)$ are the real and imaginary parts of $\nu_G\nu_{-G}$, respectively. From Eqs. (A4), (A5), and (17), we have

$$K_0'' = -(K_0'' \cos\theta_B + \mathrm{Im}\nu_0) \ , \tag{A9}$$

and clearly

$$\xi_G'' = \xi_0'' \ . \tag{A10}$$

Placing Eqs. (A9) and (A10) into (A8) and solving for K_0'', we have

$$K_0'' = -\frac{\mathrm{Im}\nu^2}{(\xi_0' + \xi_G')\cos\theta_B} - \frac{\mathrm{Im}\nu_0}{\cos\theta_B} \ . \tag{A11}$$

Thus, the absorption coefficient along the normal is

$$\mu_n = 2K_0'' = -2\frac{\mathrm{Im}\nu^2}{(\xi_0' + \xi_G')\cos\theta_B} + \frac{\mu_0}{\cos\theta_B} \ , \tag{A12}$$

where the isotropic absorption coefficient, when the crystal is oriented far from a Bragg condition, is $\mu_0 = -2\,\mathrm{Im}\nu_0$. If the absorption is not too strong, we can neglect the term $\xi_0''\xi_G''$ in Eq. (A7). Then our results for $Q - K_0 = \xi_0$ and $Q - K_G = \xi_G$ in Sec. III are valid if we replace $\xi_0 \approx \xi_0'$ and $\xi_G \approx \xi_G'$. Using Eqs. (21a), (21b), (29), and (30), we have

$$\xi_0' + \xi_G' = \pm 2\,\mathrm{Re}(\nu^2)(1 - p^2)^{-1/2} \ . \tag{A13}$$

The absorption coefficient μ_j along the trajectory is related to μ_n by

$$\mu_j = \mu_n(\hat{x} \cdot \hat{j}) \ . \tag{A14}$$

Using Eq. (25), we have

$$\hat{x} \cdot \hat{j} = (p^2 \tan^2\theta_B + 1)^{-1/2} \ . \tag{A15}$$

Therefore, the probability for absorption per unit path length along the trajectory is

$$\mu_j = \frac{\mu_0}{\cos\theta_B}\left[1 \mp \frac{\mathrm{Im}\nu^2}{\mathrm{Re}\nu^2}\frac{1}{\mu_0}(1 - p^2)^{1/2}\right]$$
$$\times (p^2 \tan^2\theta_B + 1)^{-1/2} \ . \tag{A16}$$

The upper $(-)$ sign refers to the β branch, and the lower $(+)$ sign refers to the α branch. Writing

$$\nu_G = \nu_G' + i\nu_G'' \ , \tag{A17}$$

we have in general

$$\nu^2 = \nu_G\nu_{-G} = \nu_G'\nu_{-G}' - \nu_G''\nu_{-G}'' + i(\nu_G''\nu_{-G}' + \nu_{-G}''\nu_G') \ . \tag{A18}$$

Thus, for a Bravais lattice, the ratio

$$C_0 \equiv \frac{\mathrm{Im}\nu^2}{\mu_0\,\mathrm{Re}\nu^2} = -1 \ . \tag{A19}$$

These results are well known in the case of the dynamical diffraction of x rays (see, for example, the article by Batterman and Coles).

---

[1]C. G. Shull, Phys. Rev. Lett. 21, 1585 (1968).

[2]For an introduction to the dynamical theory of neutron diffraction, see C. Stassis and J. A. Oberteuffer, Phys. Rev. B 10, 5192 (1974); V. F. Sears, Can. J. Phys. 56, 1261 (1979); H. A. Rauch and D.Petrascheck, in *Neutron Diffraction,* edited by H. Dachs, (Springer, Berlin, 1978), pp. 303–351; or G. L. Squires, *Thermal Neutron Scattering* (Cambridge U. P., Cambridge, England, 1978), pp. 116–128. There are many excellent reviews of the dynamical theory of x-ray diffraction. For example: B. W. Batterman and H. Cole, Rev. Mod. Phys. 36, 681 (1964); R. W. James, Solid State Phys. 15 (1963). N. Kato, in *X-Ray Diffraction,* edited by L. V. Azaroff (McGraw-Hill, New York, 1974), Chaps. 3 and 4; Z. G. Pinsker, *Dynamical Scattering of X Rays in Crystals* (Springer, Berlin, 1977); and W. H. Zachariasen, *Theory of X-ray Diffraction in Crystals* (Wiley, New York, 1945).

[3]U. Bonse and M. Hart, Appl. Phys. Lett. 6, 155 (1965).

[4]The first demonstration that the Bonse-Hart interferometer would work for neutrons was achieved by H. Rauch, W.

Treimer, and U. Bonse, Phys. Lett. A 47, 425 (1974). For a recent review of x-ray and neutron interferometry see the article by U. Bonse and W. Graeff, in *X-Ray Optics,* edited by H.-J. Queisser (Springer, Berlin, 1977), Vol. 22, pp. 93–143; and *Proceedings of the Conference on Neutron Interferometery, Institute Laue-Langevin, Grenoble, France, June 1978,* to appear in *Neutron Interferometry,* edited by U. Bonse and H. Rauch (Oxford, U.P., New York, in press).

[5]H. Rauch and D. Petrascheck, in *Neutron Diffraction,* edited by H. Dachs (Springer, Berlin, 1978), pp. 303–351.

[6]R. Colella, A. W. Overhauser, and S. A. Werner, Phys. Rev. Lett. 34, 1472 (1975); S. A. Werner, R. Colella, A. W. Overhauser, and C. F. Eagen, in *Proceedings of the International Conference on Neutron Scattering, Gatlinburg, Tennessee, 1976* (unpublished), pp. 1060–1072.

[7]S. A. Werner, R. Colella, A. W. Overhauser, and C. F. Eagen, Phys. Rev. Lett. 35, 1053 (1975); H. Rauch, Z. Zeilinger, G. Badurek, A. Wilfing, W. Bauspiess, and U. Bonse, Phys. Lett. A 54, 425 (1975).

[8]S. A. Werner, J.-L. Staudenmann, and R. Colella, Phys. Rev. Lett. 42, 1103 (1979).

[9]See, for example, B. W. Batterman and H. Cole, Rev. Mod. Phys. 36, 681 (1964).

[10]G. H. Wannier, Rev. Mod. Phys. 34, 645 (1962).

[11]N. Kato, J. Phys. Soc. Jpn. 18, 1785 (1963); 19, 67, 971 (1964).

[12]P. Penning and D. Polder, Philips Res. Rep. 16, 419 (1961).

[13]S. Takagi, Acta Crystallogr. 15, 1311 (1962); J. Phys. Soc. Jpn. 26, 1239 (1969).

[14]D. Taupin, Bull. Soc. Franc. Mineral Crist. 84, 51 (1961).

[15]T. Katagawa and N. Kato, Acta. Crystallogr. A 30, 830 (1974).

[16]See, for example, in *Handbook of Mathematical Functions,* edited by M. Abramowitz and I. A. Stegun (Dover, New York, 1964).

[17]N. Kato, J. Phys. Soc. Jpn. 21, 1160 (1966); Acta Crystallogr. A 25, 115 (1969); 14, 526, 627 (1961); J. Appl. Phys. 39, 2225, 2231 (1968).

[18]Z. Zeilinger and C. G. Shull, Phys. Rev. B (in press).